Combined interferometric and absorption-spectroscopic technique for determining molecular line strengths: Applications to CO_2

A. Castrillo, G. Gagliardi, G. Casa, and L. Gianfrani*
Dipartimento di Scienze Ambientali, Seconda Università di Napoli, and INFM–Gruppo Coordinato Napoli 2, Via Vivaldi 43, I-81100 Caserta, Italy

(Received 22 October 2002; published 17 June 2003)

A diode-laser-based technique has been developed for absolute line strength measurements with high precision and accuracy, combining a spectroscopic determination of the integrated absorbance with an optical measurement of the absorption path length by means of a Michelson interferometer. This method has been applied to several $^{12}C^{16}O_2$ vibrorotational transitions belonging to the $\nu_1+2\nu_2^0+\nu_3$ combination band, in the spectral region around 2 μm. The 1σ overall accuracy in line strength determination ranges between 0.4% and 0.7%, while the experimental reproducibility is estimated to be around 0.1%. To our knowledge, these levels are the highest ever reached before. The pressure-broadening coefficients for the same transitions are also reported.

DOI: 10.1103/PhysRevA.67.062503 PACS number(s): 33.70.Fd, 33.20.Ea, 42.62.Fi

I. INTRODUCTION

The measurement of the absolute intensity of molecular spectral lines is of great importance for a large variety of applications in different research fields, including astrophysics, atmospheric chemistry, and meteorology. This is the reason why so many efforts have been done, in the past few decades, in the attempt to quantify the absorption features of several gaseous species. A large amount of spectroscopic data has been collected in the HITRAN database [1], which has been widely recognized as a good compendium for many molecules. Like other databases, it is made of a proper combination of laboratory measurements and quantum-mechanical calculations, most of the information on weaker bands coming from theoretical extrapolations of data on stronger bands. Nonetheless, the accuracy is not sufficient, in many cases, even when experimental data are available. This is especially true for some molecular species, such as CO_2, H_2O, CH_4, and NH_3, of crucial importance for studies of planetary atmospheres [2]. Indeed, the characterization of their molecular composition is often limited by the lack of quantitative spectroscopic data. Furthermore, the accurate knowledge of spectroscopic parameters in the near-infrared region is often indispensable in order to retrieve gas concentrations with high accuracy, when diode laser-based spectrometers are used for *in situ* or remote monitoring of Earth's atmosphere [3,4].

Absorption spectroscopy based on room-temperature, distributed feedback (DFB), semiconductor diode lasers in the near-infrared enables the observation of molecular lines with high-resolution, experimental reproducibility and accuracy [5,6]. It is well known that InGaAs/InP diode lasers may probe vibrorotational transitions belonging to overtone and combination bands in the spectral region between 0.7 and 2.0 μm. A simple and powerful approach to retrieve absolute line intensities of a certain molecular species is based on Beer-Lambert's law and relies on the measurement of the integrated absorbance, when both the absorption path length and the gas concentration are known [7]. Basically, a high-precision level can be achieved in this way but the accuracy is usually limited by several factors, including the uncertainty on the absorption path length through the sample gas.

In this paper, we report on a novel experimental approach for high precision and accuracy measurement of absolute line intensities. It was successfully applied to six CO_2 transitions, belonging to the $\nu_1+2\nu_2^0+\nu_3$ combination band, around 5000 cm^{-1}. This spectral feature attracts a lot of interest among the spectroscopic community, providing the most advantageous way to develop on-line CO_2 sensors, based on diode lasers, for combustion applications [8], volcanic gas monitoring [9], and greenhouse effect studies [10]. Most of the available data on this band were obtained using Fourier transform (FT) spectrometers [11–13] and, more recently, a diode laser spectrometer [7], with relative uncertainties ranging between 2% and 10%.

A significant improvement in the accuracy was achieved in the present work combining the direct observation of the absorption line shape in a sample cell with the measurement of the absorption path length, by means of a Michelson interferometer. The experimental results are discussed and compared with previous data, also including those reported in the HITRAN database.

II. EXPERIMENTAL APPARATUS

A sketch of the experimental arrangement is shown in Fig. 1. A DFB diode laser, emitting 2 mW cw at 1.999 μm, was used as a tuneable laser source. The emission linewidth was about 10 MHz. The laser was driven by a low-noise current supply, while its temperature was stabilized within 1 mK by means of a temperature controller. Coarse and fine tunings of the wavelength were made changing the laser temperature and injection current, with a rate of about 1.2 Å/K and 0.9 GHz/mA, respectively.

The laser beam was directed to a 10-cm-long sample cell,

*Corresponding author. Email address: livio.gianfrani@na.infn.it; Fax: ++39-0823-274605.

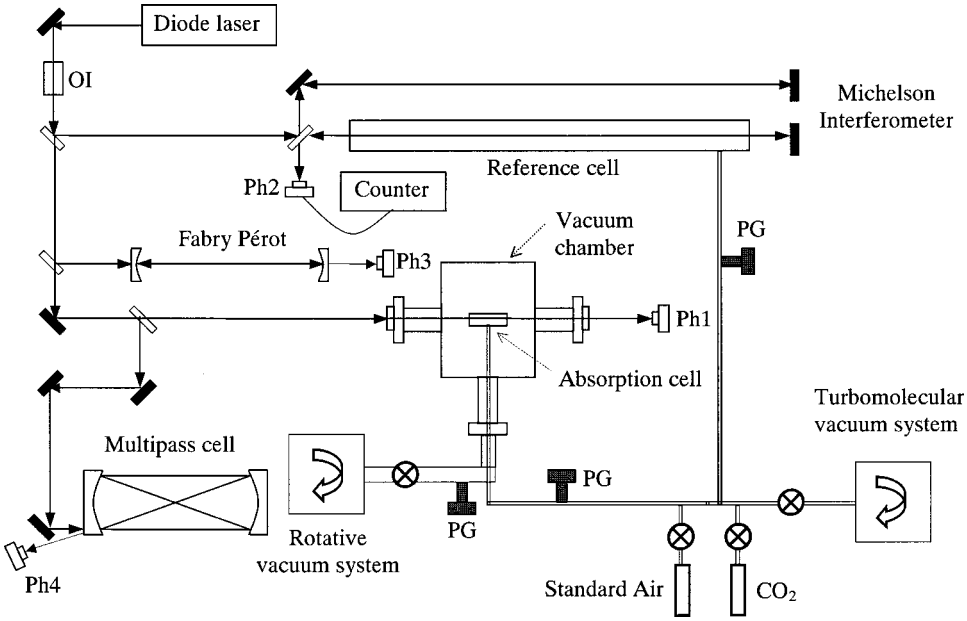

FIG. 1. Sketch of the experimental setup. DL stands for diode laser, PG for pressure gauge, Ph for photodiode, and OI for optical isolator. The sample cell is placed in a vacuum chamber to ensure a good thermal insulation. A Michelson interferometer is used to measure the beam path length in the reference cell.

filled with pure CO_2 gas (99.99%) at adjustable pressure, which was measured using a 100- and a 1000-Torr full-scale capacitance gauge with a 0.25% accuracy. In order to maintain the gas temperature constant during the whole measurement time, the cell was placed into a vacuum chamber equipped with two antireflection-coated BK7 windows. The cell temperature was monitored using a *K*-type thermocouple with a 0.1-K accuracy. A vacuum system, based on a turbomolecular pump, ensured high purity in the sample gas cell, while a rotative pump provided the vacuum inside the chamber. The transmitted radiation was focused onto a room-temperature InGaAs photodiode (Ph1), whose output signal was preamplified and sent to a digital oscilloscope for data acquisition. Signal averaging allowed us to increase the signal-to-noise ratio, reducing the detection bandwidth down to about 100 Hz. The acquired spectra were transferred to a personal computer, through a GPIB board, with a total number of 500 points for each spectrum and a 16-bit vertical resolution. The laser frequency was linearly scanned over the absorption line shape by means of a triangular modulation of the injection current in the range between 70 and 90 mA, to cover a spectral interval as wide as 20 GHz, at a rate of about 5 Hz. A small portion of the laser beam was coupled to a 50-cm-long confocal Fabry-Pérot interferometer that provided frequency markers for precise frequency calibration of the absorption spectra. The free-spectral range (FSR) was measured to be (149.6 ± 0.7) MHz. This value was carried out using pairs of $^{12}CO_2$ and $^{13}CO_2$ lines as references, whose line-center frequencies were taken from the HITRAN database.

As will be explained in Sec. III B, the spectral purity of the laser emission was carefully examined in order to prevent that the presence of laser cavity extra modes could affect the measurements. For this purpose, a further portion of the beam was directed to a Herriott-type multiple reflection cell, providing an optical path length of 30 m. It enabled us to measure the 100% absorption level in correspondence with the line center of each vibrorotational line investigated in this work.

A Michelson interferometer was employed to determine the absorption path length in the sample cell. In one of its arms, a 1-m-long absorption cell was placed and used as a reference cell. This cell could be filled with standard air, depleted in H_2O and CO_2 (at a level of 5 and 1 ppm, respectively), at adjustable pressure. Also in this case, the cell was equipped with an absolute pressure gauge and a *K*-type thermocouple, for the precise determination of the thermodynamic conditions of the inside gas. Sliding of interference fringes was monitored using an InGaAs preamplified photodiode (Ph2) and counted by a universal counter. An uncertainty of half a fringe was achieved, using a half-wave rectifier circuit on the output stage of the photodiode to drive the counter.

III. MEASUREMENT PROCEDURE

The measurement procedure relies on the precise detection of the attenuation of coherent radiation by CO_2 molecules for given frequencies, corresponding to vibrorotational transitions. The absorption process occurring in the sample cell is ruled by the well-known Beer-Lambert law, which states that the transmitted power P decreases as

$$P(\nu) = P_0 \exp[-S(T) g(\nu - \nu_0) LN], \tag{1}$$

where P_0 is the incident power, ν is the laser frequency (in cm^{-1}), ν_0 is the line-center frequency, L is the absorption path length (in cm), N is the gas density (in molecules cm^{-3}), S is the transition strength (in cm/molecule), which is a function of the gas temperature T, and $g(\nu - \nu_0)$ is the normalized line-shape function (in cm). This function is generally a Voigt profile that accounts for both Doppler and collision broadening mechanisms. From Eq. (1), one can derive a simple expression for the integrated absorbance A, that is,

$$A = \int \ln[P_0 / P(\nu)] d\nu = S(T) LN, \tag{2}$$

which represents our observable in the recorded spectra. Since the CO_2 number density can be derived from the measurement of the gas temperature and pressure, the transition strength S can be readily determined, using Eq. (2), if L is known.

A. Measurement of the absorption path length

The measurement of the absorption path length in the sample cell is based on a very accurate interferometric method. As mentioned above, a 1-m-long reference cell was placed in one arm of a Michelson interferometer. After evacuating the cell, the standard air sample was slowly injected up to a pressure of (908.0 ± 0.1) Torr, thus causing the refractivity, $(n-1)$, to change from 0 up to $(3.3335 \pm 0.0004) \times 10^{-4}$. As a consequence, during the time interval of about 5 min in which the gas pressure increased, a movement of the interference fringes could be observed and carefully quantified. The change in the optical-path difference between the two arms, Δl, and the corresponding total number of fringes, F, which followed one another on the photodetector Ph2, are related by the following expression [14]:

$$\Delta l = (n_f - 1) L_0 = F \frac{\lambda}{2}, \tag{3}$$

λ being the laser wavelength, n_f the refractive index of air at the final value of the air pressure, and L_0 the reference cell length. The refractivity of air, as a function of the wavelength as well as of gas composition, partial pressures, and temperature, was provided by the updated Edlén formula [15]:

$$n - 1 = \frac{p \times 10^{-8} [8342{,}54 + 2406147(130 - \sigma^2)^{-1} + 15998(38{,}9 - \sigma^2)^{-1}][1 + 10^{-8} \times (0{,}601 - 0{,}00972t)p]}{96095{,}43(1 + 0{,}003661t)}, \tag{4}$$

where p and t are the air pressure and temperature in Pa and °C, respectively, while σ is the wave number in μm^{-1}. Further corrections due to the presence of small amounts of H_2O and CO_2 were taken into account using the expressions reported in Ref. [15]. Also, the use of a long path cell in conjunction with the half-fringe counting system enabled us to achieve a good precision in the interferometric measurement, the relative uncertainty on F being 0.08%. Using Eq. (3), we found $L_0 = (1.0155 \pm 0.0003)$ m. This value represented our reference optical length, to which the absorption path length in the sample cell, L, had to be compared. In fact, L was retrieved from the integrated absorbances, A_S and A_R, measured in the sample and reference cells, respectively, in the presence of CO_2 gas samples at the same thermodynamic conditions. Particularly, one obtains from Eq. (2)

$$L = L_0 \frac{A_S}{A_R}. \tag{5}$$

The ratio A_S/A_R was measured for the $R(30)$ line at three different pressures, namely 50, 100, and 150 Torr, 30 repeated measurements having been performed in each case. The procedure of spectra analysis, providing the integrated absorbance, will be explained in the next section. As a result of the statistical analysis of the A_S/A_R values, we found $L = (0.104\,22 \pm 0.000\,03)$ m.

The absorption length was also retrieved from the acquired spectra using a different approach based on the measurement of the fractional absorption at the line center, instead of the integrated absorbance. The L value, carried out in this case, was in total agreement with that reported above.

B. Determination of the integrated absorbance

The absorption profile for a given vibrorotational transition was recorded as a function of the CO_2 pressure inside the sample cell, in the range between 30 and 300 Torr. After each sample injection, a time interval of about 10 min was needed in order to let the gas reach the thermal equilibrium. Also, the transmitted power from the Fabry-Pérot interferometer was simultaneously detected, in order to calibrate the laser frequency scan. The absorption spectra were carefully analyzed using a MATLAB code. This procedure consisted of a nonlinear least-squares fit of the line profiles to Eq. (1), based on the Levenberg-Marquardt routine. A fourth-order polynomial dependence of P_0 on the laser frequency was considered to take into account the laser power modulation, which occurred during the laser current scans. Furthermore, the Voigt profile was expressed as the real part of the complex probability function, which could be efficiently evaluated using the Humlicek algorithm [16]. An example of the CO_2 absorption spectrum is reported in Fig. 2. The best-fit curve is also shown with the residuals in an expanded scale. It is worth noting the excellent agreement between the expected and the experimental profile, within a root-mean-square deviation of about 1.6×10^{-3}. Once the line-shape parameters were determined for a given spectrum, the integrated absorbance could be calculated numerically.

The stability of the experimental setup, as well as the high signal-to-noise ratio, enabled us to achieve an experimental reproducibility in the spectra recovering better than 0.1%. In fact, we found an overall precision in the integrated absorbance determination ranging between 0.07% and 0.16%, depending on the line. These values, corresponding to one standard deviation, were carried out over 30 spectra acquisitions repeated in the same experimental conditions. The main source of error was due to the uncertainty in the frequency calibration of the laser scans. Taking into account the maximum uncertainty on the FSR of the Fabry-Pérot interferometer, we estimated an error on the integrated absorbance of 1%. Systematic errors due to possible distortions in the ob-

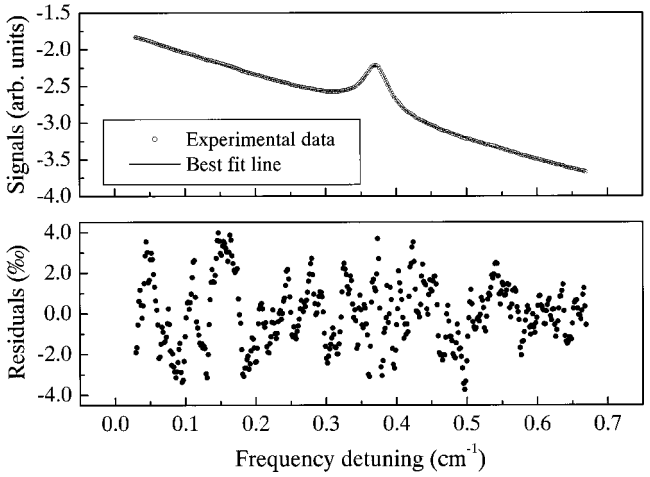

FIG. 2. Example of a CO_2 absorption profile, in correspondence of the $R(40)$ line of the $\nu_1+2\nu_2^0+\nu_3$ combination band, at 5003.445 cm^{-1}. The theoretical line shape, given by a Voigt convolution, is also shown. Residuals are reported in the bottom part of the figure and exhibit a root-mean-square value of 0.16%.

served line profile could be neglected, the linearity in the laser frequency scan being better than 0.1%. Another source of systematic error was singled out in the spectral purity of the diode laser itself and could be eliminated. Indeed, the diode laser spectral emission was carefully examined by means of the Fabry-Pérot interferometer and the presence of weak extra laser modes could be evidenced, with a side-mode suppression ratio ranging from a few ‰ up to 1%, depending on the laser operating conditions. The coexistence of different laser modes may give rise to a false zero. Namely, the optical zero, which is observed when a 100% absorption of the main laser mode takes place, does not result in a zero detected signal. In our case, since the power delivered on each mode was well defined and reproducible, the optical zero could be accurately evaluated. Figure 3 shows an example of a CO_2 absorption line under saturation conditions, observed in the multiple reflection cell at a pressure of 4 Torr. The optical zero level can be compared to the dark signal coming from the detector. It is worth noting that the optical zero had to be scaled by a factor given by the

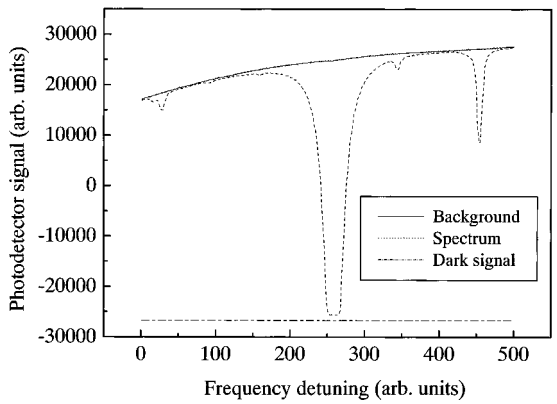

FIG. 3. Example of a CO_2 line with 100% of absorption for the determination of the optical zero.

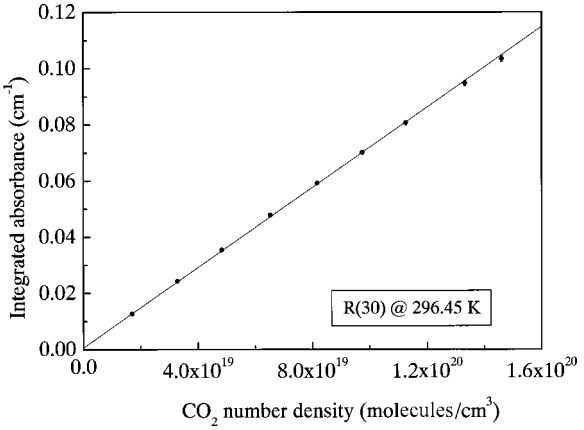

FIG. 4. Integrated absorbance data as a function of the CO_2 number density, for the $R(30)$ line. The slope of the best-fit line provides the product between the line strength and the absorption path length.

ratio of the incident powers upon the sample and multipass cells, before being considered in the spectra analysis. This correction increased the integrated absorbance by an amount ranging from 0.3% to 3%.

IV. RESULTS AND DISCUSSION

In this experiment, we focused our attention on the R branch of the $\nu_1+2\nu_2^0+\nu_3$ vibrational band, which takes place between 4950 and 5010 cm^{-1}, with line intensities typically ranging from 10^{-21} to 10^{-24} cm/molecules. In particular, we measured the line strength of six lines, going from $R(30)$ to $R(40)$, over a 5-cm^{-1}-wide spectral interval.

In Fig. 4, the integrated absorbance data for the $R(30)$ are shown as a function of the gas number densities, which were calculated from the pressure and temperature values. According to Eq. (2), the line strength S was determined from the slope of a weighted linear fit, taking into account the errors on both the variables. In Table I, the measured S values are reported along with the corresponding uncertainties. It is worth noting that the total relative uncertainty ranges between 0.4% and 0.7%. To summarize, we considered the errors on the frequency calibration (affecting the A values), on the gas pressure and temperature (propagated on the N values), as well as the error on the measured absorption path length, while the errors coming from the repeatability of the experimental results could be neglected. Thanks to the Michelson interferometer, the accuracy of the measured line strengths was no longer limited by the knowledge of the absorption path length but instead was limited mainly by the accuracy in the frequency calibration. On the other hand, the plot in Fig. 4 shows a nearly perfect agreement between the experimental points and the linear fit, which was observed for all the investigated lines. This is also due to the passive temperature stabilization system of the sample gas cell, which turned out to be very efficient. Indeed, the gas temperature was observed to be stable within the accuracy of the thermometer, during each series. Small variations were observed only from one series to another, the measured temperature values being reported in the third entry of Table I. The line-strength values, normalized at the reference temperature $T_0=296$ K, are

TABLE I. Experimental results.

Line	S (10^{-22} cm/molecule)	T (K)	S at 296 K (10^{-22} cm/molecule)	$\|R\|^2$ (10^{-6} Debye^2)	Self-broadening coefficient (cm^{-1}/atm)
$R(30)$	6.85 ± 0.04	296.45	6.85 ± 0.04	9.00 ± 0.05	0.174 ± 0.011
$R(32)$	5.95 ± 0.03	296.85	5.95 ± 0.03	9.32 ± 0.05	0.169 ± 0.010
$R(34)$	4.82 ± 0.03	297.05	4.82 ± 0.03	9.17 ± 0.06	0.169 ± 0.014
$R(36)$	3.92 ± 0.03	297.15	3.91 ± 0.03	9.22 ± 0.07	0.167 ± 0.012
$R(38)$	3.054 ± 0.017	297.35	3.051 ± 0.019	9.05 ± 0.06	0.155 ± 0.010
$R(40)$	2.394 ± 0.014	297.35	2.387 ± 0.014	9.08 ± 0.05	0.150 ± 0.010

reported in the fourth entry of the table. They have been calculated from the data in the second column using the following expression:

$$S(T)=S(T_0)\frac{Q(T_0)}{Q(T)}\left(\frac{T_0}{T}\right)\exp\left[-hc\frac{E''}{k_B}\left(\frac{1}{T}-\frac{1}{T_0}\right)\right]\times\left[1-\exp\left(-\frac{hc\nu_0}{k_BT}\right)\right]\left[1-\exp\left(-\frac{hc\nu_0}{k_BT}\right)\right]^{-1}, \quad (6)$$

$S(T_0)$ being the line strength at the reference temperature and E'' the lower state energy of the transition. The CO_2 partition function $Q(T)$ can be well approximated by the polynomial $a+bT+cT^2+dT^3$ (with $a=-1.3617$, $b=0.948\,99$, $c=-0.692\,59\times10^{-3}$, and $d=0.259\,74\times10^{-5}$) [17]. Furthermore, the normalized line strength values, as well as $Q(T_0)$, were used to calculate the square of the transition dipole moments, which are reported in the fifth column of Table I.

We made a comparison with the line strength values reported in previous papers and with the HITRAN database [1]. In particular, we considered the work performed by Valero *et al.* for several transitions of the same band, by means of an FTIR spectrometer [12], and that by Corsi *et al.*, using diode laser spectroscopy [7]. In Fig. 5, these values are compared with our data. It is worth noting that our results are in good agreement with the values reported by Valero *et al.*, as well as with those reported in the HITRAN database, but much more accurate. Indeed, the experimental results in Ref. [12] present an overall estimated accuracy (also including possible systematic errors) of about 2%, while the error code in the HITRAN database suggests an uncertainty between 2% and 5%. On the other hand, the same absolute intensities, as provided by Corsi *et al.*, are shifted towards smaller values, even though they still agree with our data because of their large errors, always greater than 4% [7].

As a result of the nonlinear least-squares fit of the absorption spectra, we also determined the homogeneous linewidth. In order to check the correctness of our data analysis procedure, for each line, the integrated absorbance data were plotted as a function of the homogeneous linewidths, both retrieved from the absorption spectra at different pressures. A linear correlation between the two sets of data is obviously expected. Indeed, we found excellent values of the linear regression coefficient for the data sets related to all the investigated lines. For instance, for the $R(30)$ data, we found a linear regression coefficient of 0.9998. Furthermore, we determined the collision self-broadening coefficients, which are reported in the sixth column of Table I. Most of these results are consistent with those reported in the HITRAN database, while in poor agreement with the data of Ref. [7], as shown in Fig. 6. Here, we may note that, although the trends of the pressure-broadening coefficient as a function of the rota-

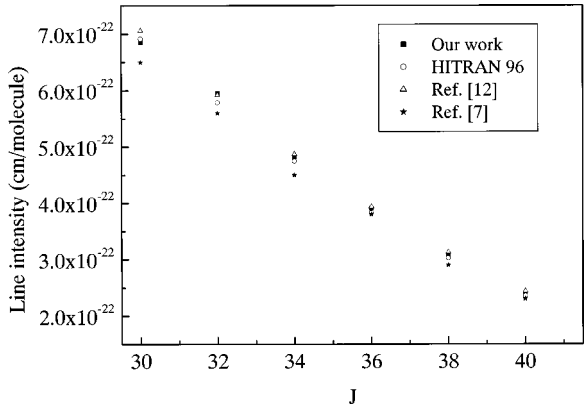

FIG. 5. Comparison between our intensity values and those reported in HITRAN, in Refs. [7] and [12]. For the sake of clarity, the error bars have not been drawn. However, the uncertainties in each set of values are discussed in the text.

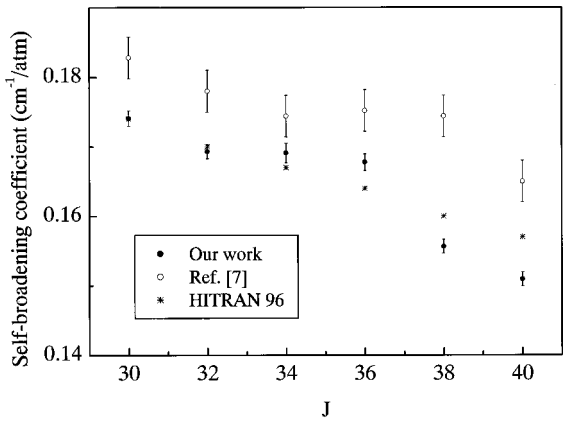

FIG. 6. Experimental self-broadening coefficients (full width at half maximum) for the lines investigated in this work. The uncertainty in the HITRAN values were not available in the 1996 edition.

tional quantum number are quite similar, the absolute values of Ref. [7] are noticeably larger than our values.

V. CONCLUSIONS

This paper represents a first important step towards the accurate determination of the absolute intensities for molecular transitions. A new approach, exploiting direct absorption spectroscopy and laser interferometry, has been successfully implemented for intensity measurements of CO_2 vibrorotational lines in the spectral region around 5000 cm^{-1}. The reproducibility of our results was about 0.1% while the accuracy varied from 0.4% to 0.7%, depending on the transition. Data already available for the same lines were found to be only in partial agreement with our results. We also provided accurate values of the transition dipole moments, which can be of particular significance in order to study the effect of the vibration-rotation interaction and clarify the puzzling situation of the Herman-Wallis factors [18].

As a result of a severe uncertainty analysis, we found that our accuracy was essentially limited by the error on the frequency scale of the recorded spectra. A drastic improvement can be achieved using two phase-locked extended-cavity diode lasers. Indeed, optical phase-locking offers the possibility to perform broad scans around an arbitrary center frequency with, in principle, a sub-Hz accuracy [19]. At the same time, the use of an extended-cavity diode laser would ensure a much better spectral purity, which would enable us to avoid the problem of the optical zero evaluation.

ACKNOWLEDGMENTS

The authors are grateful to Filippo Terrasi for helpful and stimulating discussions. This work was supported by Istituto Nazionale di Geofisica e Vulcanologia, within the framework of the GNV program 2000–2002, and by Istituto Nazionale per la Fisica della Materia.

[1] L. S. Rothmann *et al.*, J. Quant. Spectrosc. Radiat. Transf. **60**, 665 (1998).
[2] J. Geng, J. I. Lunine, and G. H. Atkinson, Appl. Opt. **40**, 2551 (2001).
[3] B. Parvitte, V. Zéninari, I. Pouchet, and G. Durry, J. Quant. Spectrosc. Radiat. Transf. **75**, 493 (2002).
[4] G. Gagliardi *et al.*, Rev. Sci. Instrum. **72**, 4228 (2001).
[5] M. Lepère, A. Henry, A. Valentin, and C. Camy-Peyret, J. Mol. Spectrosc. **208**, 25 (2001).
[6] G. Gagliardi, L. Gianfrani, and G. M. Tino, Phys. Rev. A **55**, 4597 (1997).
[7] C. Corsi, F. D'Amato, M. De Rosa, and G. Modugno, Eur. Phys. J. D **6**, 327 (1999).
[8] R. M. Mihalcea, D. S. Baer, and R. K. Hanson, Appl. Opt. **37**, 8341 (1998).
[9] L. Gianfrani, P. De Natale, and G. De Natale, Appl. Phys. B: Lasers Opt. **70**, 467 (2000).
[10] P. Werle, R. Mucke, F. D'Amato, and T. Lancia, Appl. Phys. B: Lasers Opt. **67**, 307 (1998).
[11] K. P. Vasilevskii, L. E. Danilochkina, and V. A. Kazbanov, Opt. Spectrosc. **38**, 499 (1975).
[12] F. P. J. Valero, C. B. Suarez, and R. W. Boese, J. Quant. Spectrosc. Radiat. Transf. **23**, 337 (1980).
[13] C. B. Suarez and F. P. J. Valero, J. Mol. Spectrosc. **140**, 407 (1990).
[14] W. Demtroder, *Laser Spectroscopy* (Springer-Verlag, Berlin, 1998).
[15] K. P. Birch and M. J. Downs, Metrologia **30**, 155 (1993); **31**, 315 (1994).
[16] J. Humlicek, J. Quant. Spectrosc. Radiat. Transf. **27**, 437 (1982).
[17] M. E. Webber *et al.*, in *Proceedings of the 38th AIAA Aerospace Sciences Meeting and Exhibit, Reno, 2000* (American Institute of Aeronautics and Astronautics, Reston, 2000), paper 2000-0775.
[18] C. M. Deeley and J. W. C. Johns, J. Mol. Spectrosc. **129**, 151 (1988).
[19] G. Santarelli, A. Clairon, S. N. Lea, and G. M. Tino, Opt. Commun. **104**, 339 (1994).